Ocean Modelling 80 (2014) 24–35

Contents lists available at ScienceDirect

Ocean Modelling

journal homepage: www.elsevier.com/locate/ocemod

Sensitivity of simulated global ocean carbon flux estimates to forcing by reanalysis products

Watson W. Gregg [a,*], Nancy W. Casey [b], Cecile S. Rousseaux [c]

[a] Global Modeling and Assimilation Office, NASA/Goddard Space Flight Center, Greenbelt, MD 20771, United States
[b] Science Systems and Applications, Inc., Lanham, MD 20706, United States
[c] Global Modeling and Assimilation Office, NASA/Goddard Space Flight Center, Universities Space Research Association, Greenbelt, MD 20771, United States

ARTICLE INFO

Article history:
Received 13 June 2013
Received in revised form 6 May 2014
Accepted 18 May 2014
Available online 29 May 2014

Keywords:
Reanalysis
Ocean
Carbon
Fluxes
Models

ABSTRACT

Reanalysis products from MERRA, NCEP2, NCEP1, and ECMWF were used to force an established ocean biogeochemical model to estimate air–sea carbon fluxes (FCO_2) and partial pressure of carbon dioxide (pCO_2) in the global oceans. Global air–sea carbon fluxes and pCO_2 were relatively insensitive to the choice of forcing reanalysis. All global FCO_2 estimates from the model forced by the four different reanalyses were within 20% of in situ estimates (MERRA and NCEP1 were within 7%), and all models exhibited statistically significant positive correlations with in situ estimates across the 12 major oceanographic basins. Global pCO_2 estimates were within 1% of in situ estimates with ECMWF being the outlier at 0.6%. Basin correlations were similar to FCO_2. There were, however, substantial departures among basin estimates from the different reanalysis forcings. The high latitudes and tropics had the largest ranges in estimated fluxes among the reanalyses. Regional pCO_2 differences among the reanalysis forcings were muted relative to the FCO_2 results. No individual reanalysis was uniformly better or worse in the major oceanographic basins. The results provide information on the characterization of uncertainty in ocean carbon models due to choice of reanalysis forcing.

1. Introduction

The oceans play a critical role in the global carbon cycle. More than 90% of the active non-geological carbon pool resides in the oceans (Kaufman et al., 1998). Estimates of global primary production suggest that the oceans contribute about half (Field et al., 1998). One quarter (Le Quéré et al., 2010) of the carbon emitted by anthropogenic sources is thought to be sequestered in the oceans, annually. Understanding the role of the ocean in the global carbon cycle is a driving question in modern Earth science. It requires foremost a geographically-distributed, well-maintained observational capability. We are fortunate that such a capability exists or is in development, and that global data sets of ocean carbon inventories (Key et al., 2004), partial pressure of CO_2 (Takahashi et al., 2006, 2009) and ocean-atmospheric exchange (Takahashi et al., 2006, 2009) are publicly available.

Global ocean carbon models require external information to drive the ocean circulation dynamics that determine the distributions, abundances, and atmospheric exchange of carbon. Additionally, biological and chemical constituents that play important roles in the ocean carbon cycle are affected by ocean circulation. These forcing fields can be from a coupled atmosphere model or from atmospheric and ocean data. In the latter case, the data typically come from publicly available reanalysis products (e.g., Le Quéré et al., 2010; Gorgues et al., 2010; Doney et al., 2009). It is clear that different ocean models produce different estimates of air–sea fluxes (Khatiwala et al., 2013), but less effort has been given to the influences of different reanalysis products. These differences in reanalysis products and their potential effects on simulated ocean carbon distributions and trends have been cause for concern by ocean modelers (Le Quéré et al., 2010).

Here we intercompare model air–sea flux estimates and partial pressure of carbon dioxide (pCO_2) from a model forced by four reanalysis products. These include The Modern-Era Retrospective analysis for Research and Applications (MERRA; Rienecker et al., 2011), two from the National Center for Environmental Prediction (NCEP): NCEP2 (Kanamitsu et al., 2002) and NCEP1 (Kalnay et al., 1996), and one from the European Centre for Medium-range Weather Forecasts (ECMWF; Dee et al., 2011). This study provides an opportunity to evaluate how the differences in reanalysis products propagate through the same ocean biogeochemical model to affect representations of carbon fluxes and pCO_2.

* Corresponding author. Tel.: +1 301 614 5711; fax: +1 301 614 5644.
E-mail addresses: watson.gregg@nasa.gov (W.W. Gregg), nancy.casey@ssaihq.com (N.W. Casey), cecile.s.rousseaux@nasa.gov (C.S. Rousseaux).

http://dx.doi.org/10.1016/j.ocemod.2014.05.002
1463-5003/Published by Elsevier Ltd.

This effort is potentially important not only to ocean carbon modelers, but also for reanalysis developers and analysts, satellite mission conceptual designers, and atmospheric scientists as well. The objective of this study is to provide quantitative information on the spatial distributions of air–sea carbon fluxes and ocean pCO_2 globally, regionally, and sub-regionally in a model forced by the four state-of-the-art, widely used reanalysis products listed above. Such information can guide scientists and analysts in their selection, uses, and potential pitfalls of different reanalysis products in the context of ocean carbon models.

2. Material and methods

2.1. Global three-dimensional circulation model

Global ocean carbon dynamics are simulated by the NASA Ocean Biogeochemical Model (NOBM; Fig. 1). It is a three-dimensional representation of coupled circulation/biogeochemical/radiative processes in the global oceans (Gregg et al., 2003; Gregg and Casey, 2007). It spans the domain from 84°S to 72°N latitude in increments of 1.25° longitude by 2/3° latitude, including only open ocean areas, where bottom depth > 200 m. The circulation model is quasi-isopycnal, with 14 vertical layers, driven by the forcing fields shown in Fig. 1 (Schopf and Loughe, 1995). It relaxes to sea surface temperature obtained from MERRA and surface salinity obtained from the National Oceanographic Data Center (NODC, Conkright et al., 2002). The biogeochemical processes model contains 4 phytoplankton groups, 4 nutrient groups, a single herbivore group, and 3 detrital pools. The phytoplankton groups differ in maximum growth rates, sinking rates, nutrient requirements, and optical properties. The 4 nutrients are nitrate, regenerated ammonium, silica to regulate diatom growth, and iron. Three detrital pools provide storage of organic material, sinking, and eventual remineralization.

Carbon cycling involves dissolved organic carbon (DOC) and dissolved inorganic carbon (DIC; Fig. 2). DOC has sources from phytoplankton, herbivores, and carbon detritus, and a sink to DIC. DIC has sources from phytoplankton, herbivores, carbon detritus, and DOC, and is allowed to exchange with the atmosphere, which can be either a source or sink. The ecosystem sink for DIC is phytoplankton, through photosynthesis. This represents the biological pump portion of the carbon dynamics. The solubility pump portion is represented by the interactions among temperature, alkalinity (parameterized as a function of salinity), silica, and phosphate (parameterized as a function of nitrate). The alkalinity/salinity parameterization utilizes the spatial variability of salinity in the model adjusted to mean alkalinity

$$TA = \underline{TA}\ S/\underline{S}$$

where TA is total alkalinity and S is salinity. The underscore represents global mean values. $\underline{TA}$ is specified as 2310 μE kg^{-1} (Ocean Model Intercomparison Project (OCMIP; www.ipsl.jussieu.fr/OCMIP) and $\underline{S}$ as 34.8 PSU (global model mean). Since the model contains nitrate but not phosphate, we estimate phosphate by multiplying nitrate by 0.1. This is derived from the global mean ratio of nitrate to phosphate from NODC for their top three standard levels. The calculations for the solubility pump follow the standards set by the Ocean Model Intercomparison Project (reference above). We recognize that this approximation for alkalinity is not optimal, but the surface results compare favorably with data (see Gregg et al., 2013). The difference between the model and GLODAP global surface alkalinity is 2.7 μEq l^{-1} (≈0.1%) with basin correlation of 0.95 ($P < 0.05$) (Gregg et al., 2013). We consider this sufficient for the present purpose of intercomparing model results from forcing by different reanalysis products.

We employ a locally-developed lookup table valid over modern ranges of DIC, salinity, temperature, and nutrients for computational efficiency, at little cost to accuracy. Air–sea CO_2 exchange as a function of wind uses the Wanninkhof (1992) formulation, as is common in global and regional ocean carbon models (e.g., McKinley et al., 2006). A more complete description of NOBM can be found in Gregg et al. (2013).

NOBM is spun-up for 200 years under climatological forcing from each reanalysis. Initial conditions for DIC are derived from the Global Data Analysis Project (GLODAP; Key et al., 2004). DOC initial conditions are set to 0 μM. Subsequent tests with non-zero DOC initial conditions showed negligible differences. Other initial conditions are described in Gregg and Casey (2007). For MERRA forcing, the first ten years of the run show a net pCO_2 difference ΔpCO_2 (year 10-year 1) of −0.982 μatm, at the first hundred years the 10-year ΔpCO_2 (year 100-year 91) is 0.413 μatm, and at 200 years, the 10-year ΔpCO_2 (year 200-year 191) is 0.102 μatm (Fig. 3). This 200-year model spinup may not be sufficient for full adjustment of all variables at all depths, but appears satisfactory for surface pCO_2 and nutrients, which is the focus of this effort. The results from the last year (year 200 of each reanalysis spinup) are compared with in situ data and with one another.

2.2. Data sets

2.2.1. Forcing data

Forcing data variables are shown in Fig. 1. Monthly climatologies are used in all cases. All are obtained from reanalysis products except soil dust (iron), ozone, clouds, and atmospheric CO_2. Iron is

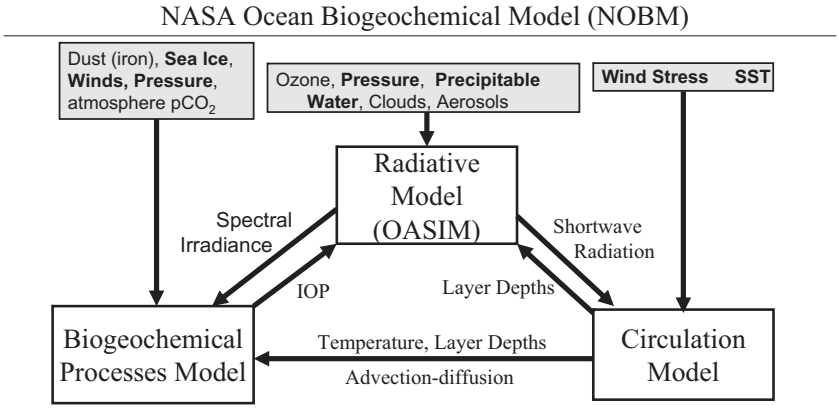

Fig. 1. Interactions among the main components of NOBM, nominal outputs, and forcing fields. IOP indicates inherent optical properties. Forcing variables are shown in the gray boxes. Reanalysis forcing variables are in bold. Surface pressure and precipitable water effects on surface irradiance play a small role in the inorganic carbon results and are ignored in this effort.

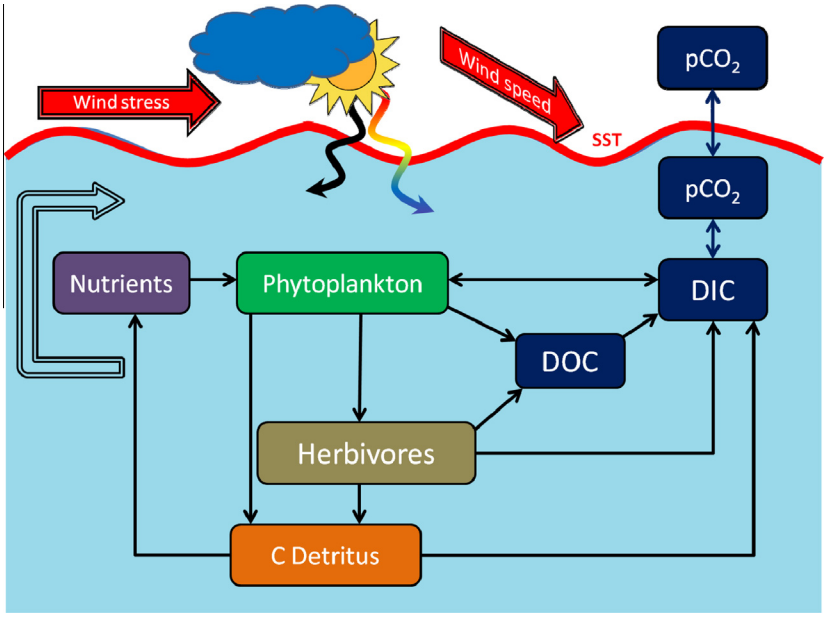

Fig. 2. Pathways and interactions among the components of the biogeochemical processes model, illustrating the interactions with the carbon cycle, comprising dissolved inorganic carbon (DIC), dissolved organic carbon and exchanges with the atmosphere as a function of the ocean and atmosphere partial pressures of CO_2 (pCO_2). The biological pump is represented by phytoplankton, herbivores, nutrients, and detritus.

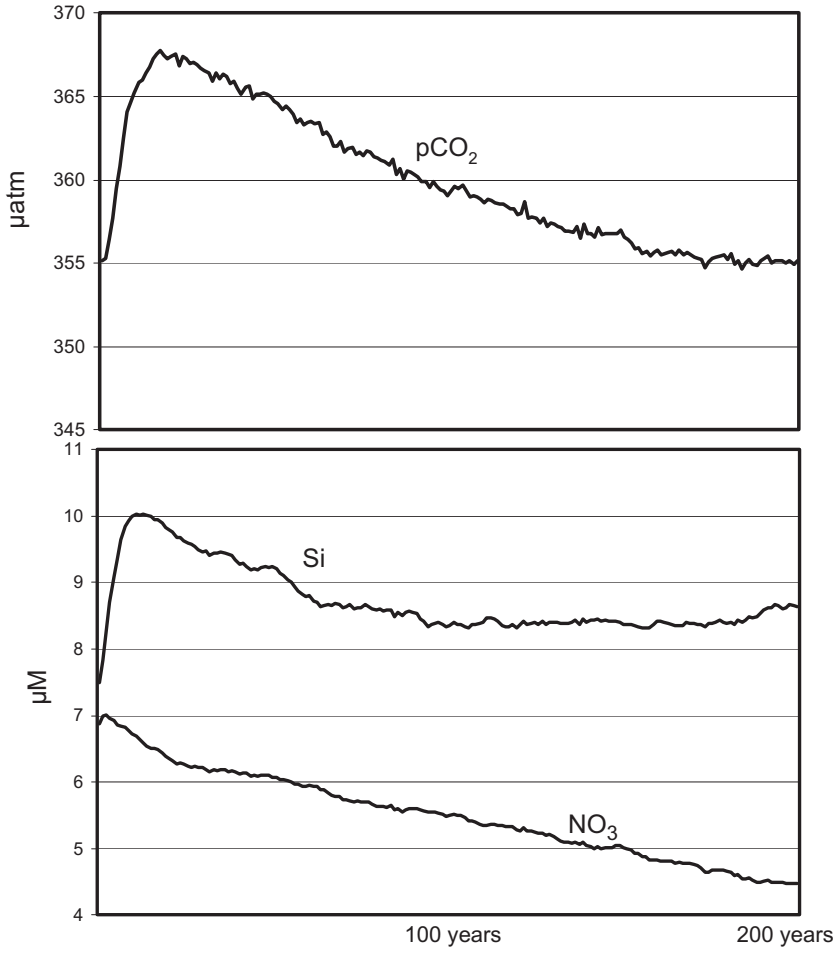

Fig. 3. Evolution of pCO_2, silicon, and nitrate global surface means over the 200-year spinup.

derived from soil dust deposition estimates from the Goddard Chemistry Aerosol Radiation and Transport model (Ginoux et al., 2001). Ozone is obtained from the Total Ozone Mapping Spectrometer and Ozone Monitoring Instrument and cloud information (specifically cloud cover and liquid water path) are obtained from the International Satellite Cloud Climatology Project. Atmospheric CO_2 is from the Lamont-Doherty Earth Observatory (LDEO) data set (Takahashi et al., 2009), using a mean over the entire range of observations of 358.7 μatm. Although the ocean pCO_2 observations are nominally normalized to the year 2000 (Takahashi et al., 2009), we keep the uncorrected mean atmospheric value from the data to represent variability at the time and location of measurement. However, tests using year 2000-normalized atmospheric pCO_2 and MERRA forcing showed a difference in air–sea fluxes of only 0.034 mol C m^{-2} y^{-1}, or about 10.3%. This produced a slightly worse comparison with in situ estimates (7.8% as compared to −2.3%), but for the present purposes consistent atmospheric pCO_2 is the important consideration.

2.2.2. Comparison data

The main output of interest in this effort is the flux of CO_2 (FCO_2, notation following Doney et al., 2009), representing the exchange of carbon between the atmosphere and ocean. Positive air–sea flux is defined here as upward, indicating a source to the atmosphere. Additionally we compare with global observations of ocean partial pressure of carbon dioxide pCO_2. Both FCO_2 and pCO_2 data sets are obtained as gridded datasets on a 5° longitude by 4° latitude horizontal grid and are surface only. They are obtained from the Lamont-Doherty Earth Observatory (LDEO) (http://cdiac.ornl.gov/oceans/LDEO_Underway_Database/index.html; Takahashi et al., 2009). The FCO_2 estimates are derived from (1) the ocean pCO_2 data using atmospheric pCO_2 to compute ΔpCO_2 which is then normalized to the year 2000, (2) wind speeds from NCEP2 and (3) an estimate of the gas transfer coefficient (see Takahashi et al., 2009).

In addition to the gridded data sets available from LDEO, shipboard underway pCO_2 data at the location of data measurement, ungridded, with temporal sampling identified, with sampling gaps preserved, and inclusive of all years sampled, are available (http://cdiac.ornl.gov/ftp/oceans/LDEO_Database/Version_2009/). Using these raw observations we can re-construct the representation of pCO_2 data at our model grid. By sub-sampling the model by the data locations, we can remove the mismatches due to data scaling, and produce a less biased, one-to-one comparison. We use these to compare with co-located, coincident estimates of pCO_2 from the MERRA model forcing version to understand the effects of gridding and sampling on the global gridded representations of pCO_2.

Carbon flux estimates are not available in the ungridded data from LDEO, but we can estimate them from pCO_2 and climatological ocean and atmospheric variables using the OCMIP protocols, similar to the way FCO_2 is computed by the model. The required variables are wind speed, sea level pressure, and atmospheric pCO_2. While all of these are derived from or force the model in the model derivation of FCO_2, we use data climatologies here to estimate FCO_2 from the LDEO pCO_2 point measurement data. The data are taken from LDEO to retain as much consistency as possible.

2.2.3. Evaluation

Results are evaluated globally and regionally in 12 major oceanographic basins (Fig. 4) from the forcing by each of the four reanalysis products. Comparisons are statistical, including differences between model global and regional means and correlation analysis. Our emphasis is on large temporal and spatial scale results, using annual area-weighted means and correlation analysis across the basins ($N = 12$, with 10 degrees of freedom). We additionally compare model pCO_2 and FCO_2 from one of the reanalyses, MERRA, against in situ data sub-regionally to estimate

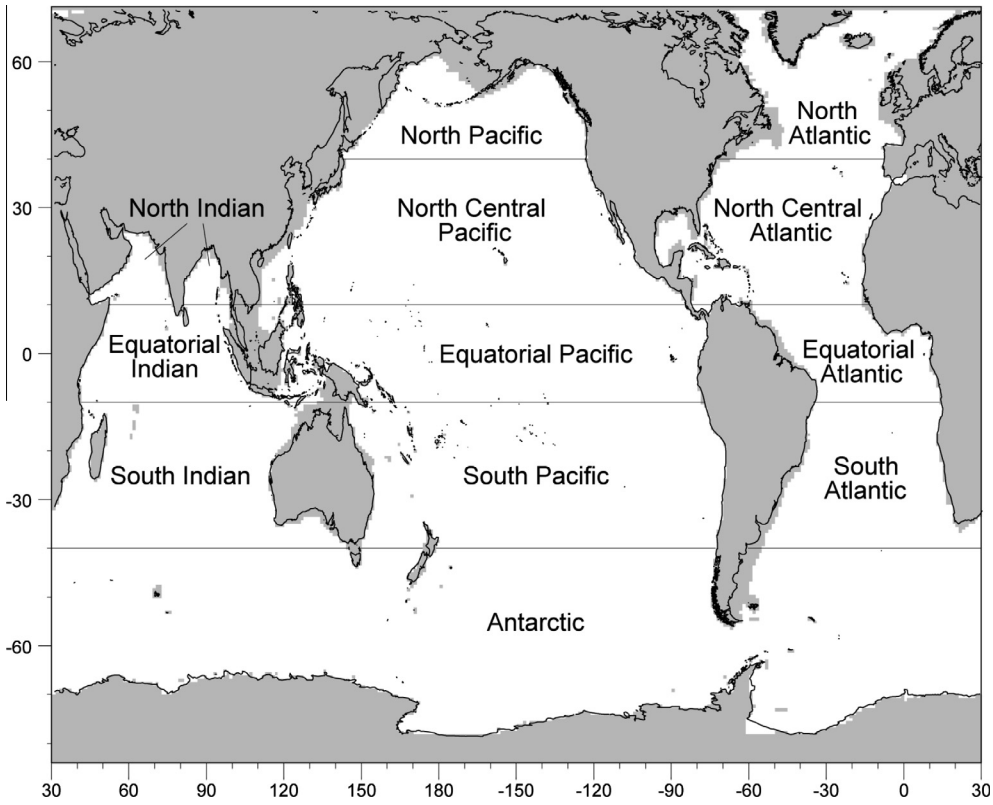

Fig. 4. Delineation of the 12 major oceanographic basins.

the influences of inherent model biases on the results shown in the intercomparison of reanalysis products.

3. Results

Global annual mean FCO_2 from the model forced by the four different reanalysis products show considerable spatial similarity (Fig. 5). The difference between the lowest estimate, NCEP2 (-0.276 mol C m^{-2} y^{-1}) and the highest, ECMWF (-0.402 mol C m^{-2} y^{-1}) is about 0.13 mol C m^{-2} y^{-1}, or about 45%. MERRA forcing is closest to in situ estimates (within 0.008 mol C m^{-2} y^{-1}, or 2%), with NCEP1 only slightly more distant (by 0.024 mol C m^{-2} y^{-1}, or 7.0%). Correlations with in situ estimates across basins are positive and statistically significant ($P < 0.05$) for all forcing, with correlation coefficient ranging from 0.73 (MERRA and ECMWF) to 0.80 (NCEP1).

There are, however, substantial differences in basin-scale estimates of FCO_2 among the various reanalysis forcings, especially in the high latitudes and tropics (Fig. 5). In the high latitudes (>±40° latitude), all the forcings produce strong sinks in the oceans, in accordance with the in situ estimates, but all are weaker than the data. The NCEP2 sink in the Antarctic is the lowest (-0.97 mol C m^{-2} y^{-1}), representing only about a third the magnitude of the next smallest sink (ECMWF). NCEP2 forcing produces an intensification and expansion of local source regions near 60°S latitude in the Antarctic (Fig. 6). This counters the amplification of the sink regions just to the north. MERRA forcing produces the smallest sink in the North Pacific and North Atlantic basins (Fig. 5). The weaker sink in the North Pacific can be attributed to a source region east of the Sea of Okhostk (Fig. 6), and the North Atlantic to a local source in the Labrador Sea. MERRA-estimated fluxes in these two basins is about 0.15 mol C m^{-2} y^{-1} (39%) lower in the North Pacific than the strongest sink and 0.33 mol C m^{-2} y^{-1} (21%) lower in the North Atlantic. The strongest sink in both cases is produced by NCEP2.

In the tropical basins, the estimates of air–sea carbon fluxes by NCEP2 produce the strongest source in 3 of the 4 major basins (Fig. 5). Sometime this is closer to the in situ estimates relative to the other forcings, as in the Equatorial Atlantic, and sometimes it is a larger departure, as in the Equatorial Indian. The large source represented by NCEP2 forcing in the Equatorial Pacific is derived from a very strong local flux along the Peru coast (Fig. 6). Although a smaller manifestation appears in NCEP1 and ECMWF forcing, it does not appear in MERRA-forcing, which leads to its representation of the smallest Equatorial Pacific source. ECMWF departs strongly from the other forcings in the North Indian, and is nearly 3 times the fluxes estimated by the lowest reanalysis (NCEP1), but is closer to the in situ estimates (Fig. 5). This stronger source can be attributed to local intensification offshore of Somalia (Fig. 6), which feature is either much smaller in the other forcings (NCEP1) or non-existent (MERRA and NCEP2).

Estimates of FCO_2 in the sub-polar basins are more similar among the forcings than the high latitudes and tropics (Fig. 5), exhibiting the lowest ranges of estimates of all the basins. ECMWF is the strongest sink in 4 of the 5 basins, while MERRA forcing is the lowest in 2 basins (North Central Pacific and Atlantic). All the forcings indicate a much stronger sink estimate in the South Atlantic and Pacific than the in situ estimates.

Global area-weighted mean partial pressures show similar relationships among the four reanalysis forcings and with the data (Fig. 7). The deviations from data are much smaller than the flux estimates: all are within 1% of data global means, with ECMWF the outlier at 0.6%. NCEP1 pCO_2 is closest to the data, with a difference < 1 μatm, or −0.1%. All forcings also show positive and statistically significant correlations across basins, with values similar to the fluxes.

On basin scales the pCO_2 mean differences between the forcings and data are smaller, and more consistent with one another than for the basin fluxes (Fig. 7). The South Atlantic is a notable exception, which exhibits a departure from the data for all forcings similar to the fluxes. NCEP2 forcing is noticeably closer to the data

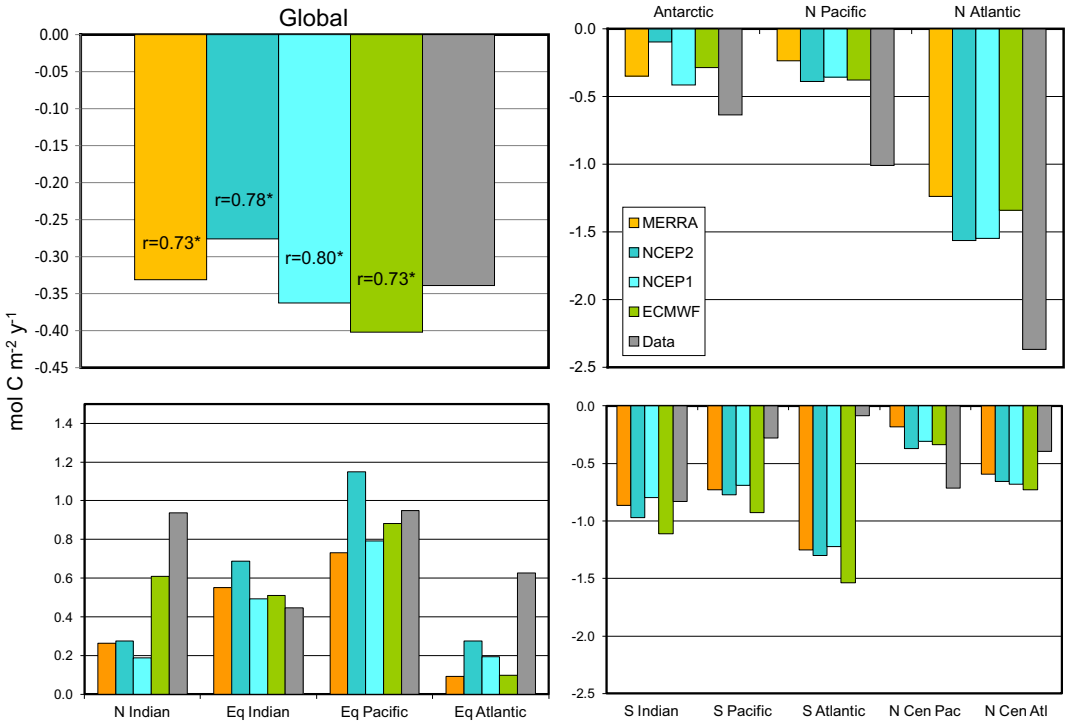

Fig. 5. Global and basin annual mean air–sea carbon fluxes (FCO_2). The basins are arranged by high latitudes (top right), tropical (bottom left), and sub-polar (bottom right). Correlation coefficients compared with in situ estimates are shown in the global plot, where an asterisk indicates $P < 0.05$.

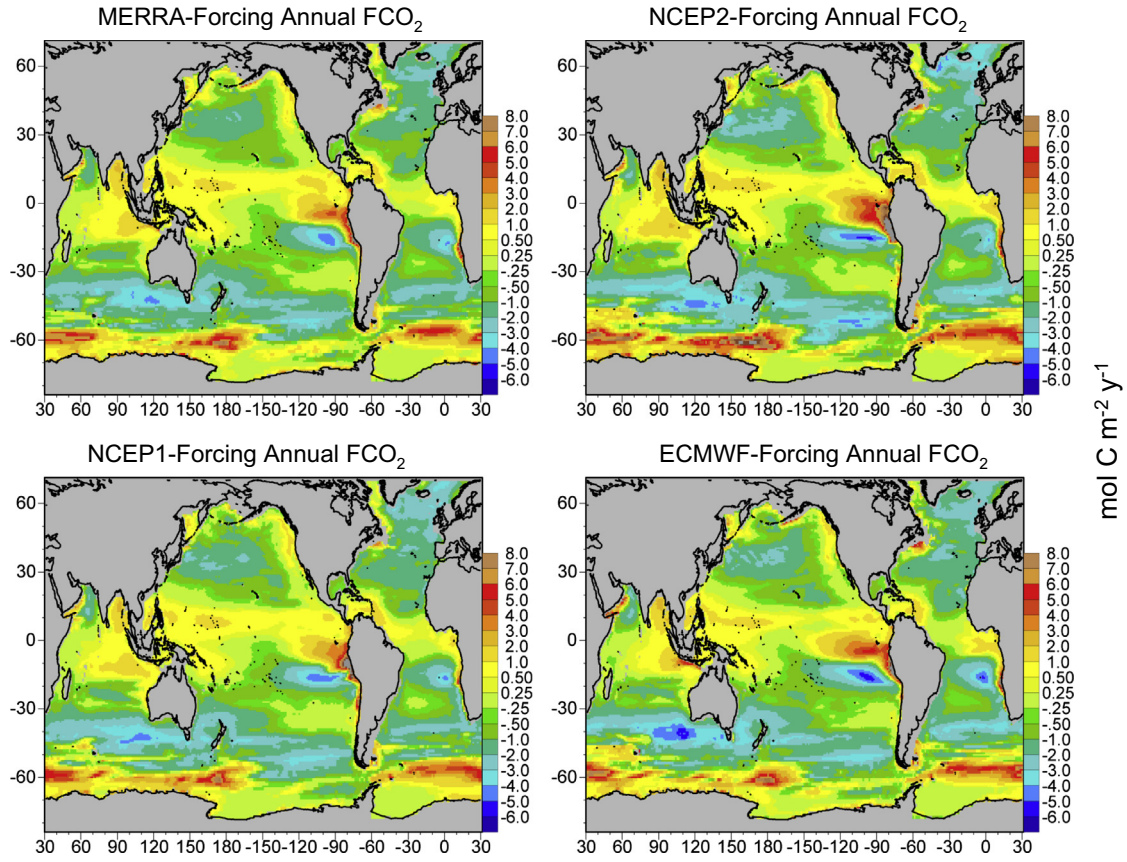

Fig. 6. Annual mean air–sea carbon fluxes (FCO_2) from the model using forcing fields from different reanalysis products.

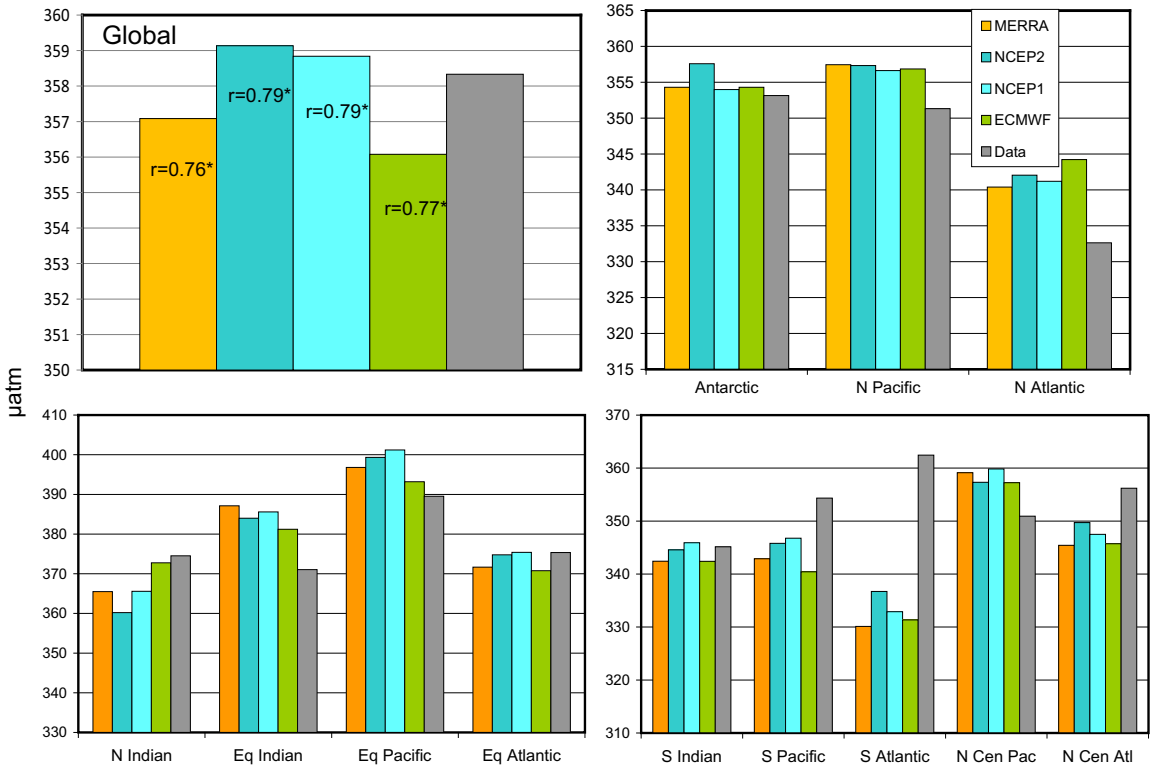

Fig. 7. Global and basin annual mean pCO_2. The basins are arranged by high latitudes (top right), tropical (bottom left), and sub-polar (bottom right). Correlation coefficients compared with in situ estimates are shown in the global plot, where an asterisk indicates $P < 0.05$.

pCO_2 but it is still low by 26 µatm (about 7%). Modeled North Atlantic pCO_2 estimates are high compared to data (maximum of 12 µatm, or 3.5%, by ECMWF). The Equatorial Atlantic estimates are consistent with data (Fig. 7), in contrast to the fluxes (Fig. 5).

Spatial distribution of pCO_2 from the different forcings generally show similar patterns as the air–sea fluxes, but the contrast between highs and lows is reduced (Fig. 8). ECMWF has the lowest pCO_2 in the southern 60° band where the fluxes are large and positive, but otherwise the features are comparable.

Selected variables from the reanalyses particularly relevant to ocean carbon surface fluxes include ice concentrations, SST, and wind speed, and are shown in Fig. 9. Differences in these reanalysis variables in the high latitude basins suggest some reasons for the differences in air–sea flux observed in the biogeochemical model (Fig. 5). Ice concentrations are similar for all four reanalyses estimates in the North Pacific and Antarctic, but there are some apparent differences in the North Atlantic. There are considerable differences in SST and wind speed among the four reanalyses for all the high latitude basins.

For the tropical basins, only SST and wind speed are shown, and there are considerable differences in the variables among the four reanalysis products (Fig. 10). NCEP2 is consistently warmer than the other reanalyses, more than 1 °C above the lowest estimate in 3 of the 4 basins, and nearly 1 °C in the North Indian. Additionally, NCEP2 always exhibits the highest annual mean wind speeds, occasionally rising to nearly 1 m s^{-1} higher than the others. At the other extreme, MERRA and NCEP1 have nearly identical annual mean SST and wind speeds in all the tropical basins. ECMWF and NCEP1 have nearly identical SST in the Equatorial Indian, Pacific, and Atlantic.

In addition to the full global representations of the model and the in situ FCO_2 gridded, re-sampled, and interpolated climatology from LDEO, we provide the non-interpolated point measurements and the corresponding model with the sampling biases of the data in time and space removed (Fig. 11). This provides a more realistic comparison of the model and data to enable improved evaluation of model issues. A difference map (Fig. 12) provides an enhancement of the comparison. A side-by-side comparison of pCO_2, both with data sampling biases and without completes the comparison (Fig. 13).

4. Discussion

4.1. Reanalysis-forcing model results

Global annual mean air–sea carbon fluxes and pCO_2 are largely independent of the choice of reanalysis forcing (Figs. 5 and 7). The flux estimates are similar, the sign of the fluxes (source or sink) by basin are identical, and correlations with in situ estimates across major oceanographic basins are positive and statistically significant ($P < 0.05$) regardless of the reanalysis forcing used. Correlations for pCO_2 are similarly positive and significant. The maximum variability in fluxes is about ±20%, which suggests the magnitude of uncertainty in ocean carbon models due to choice of reanalyses.

That global air–sea carbon fluxes and pCO_2 are generally similar regardless of reanalysis forcing is reassuring. It suggests that at the largest spatial scales, state-of-the-art representations of physical processes and assimilation approaches embedded in the reanalysis methods, while quite different among the different reanalyses, produce consistent results. In essence, this means that important variables used for ocean carbon model forcing are similar on global scales, and that whatever important differences there are among

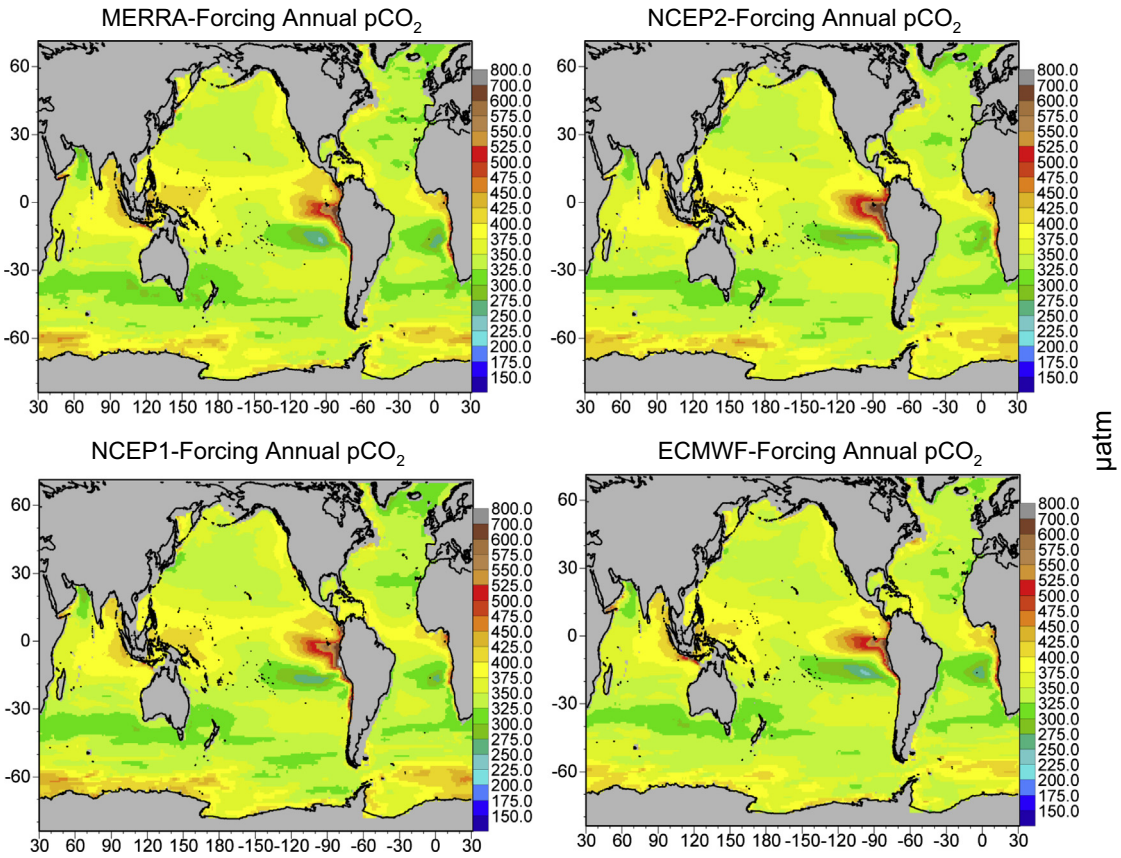

Fig. 8. Annual mean pCO_2 from the model using forcing fields from different reanalysis products.

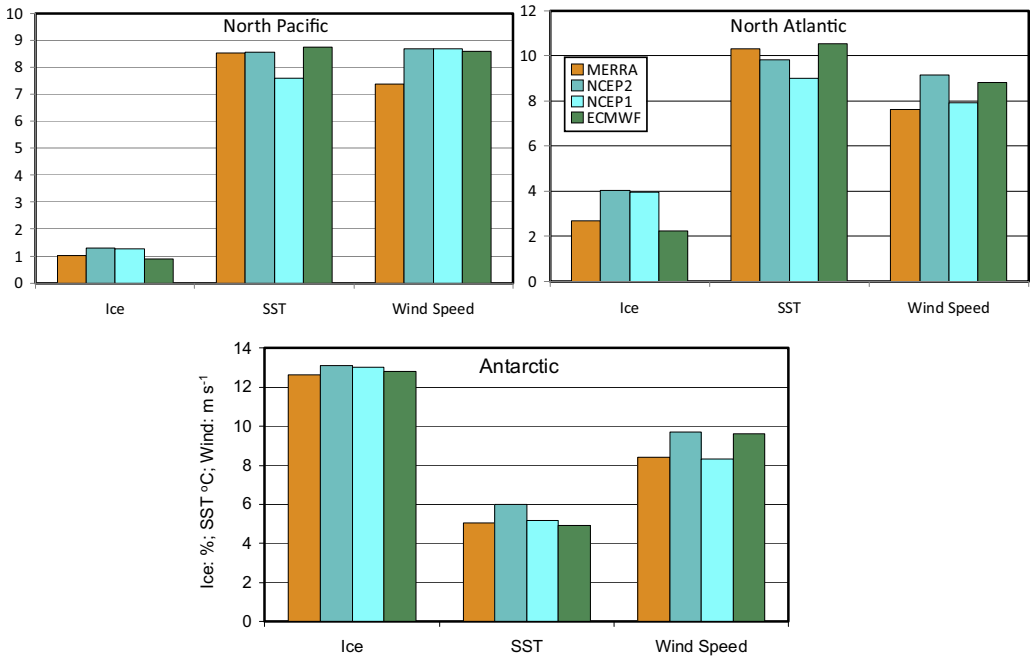

Fig. 9. Annual mean ice concentration (percent), SST (degrees C), and wind speeds (m s^{-1}) for the 4 reanalysis products in the high latitude basins.

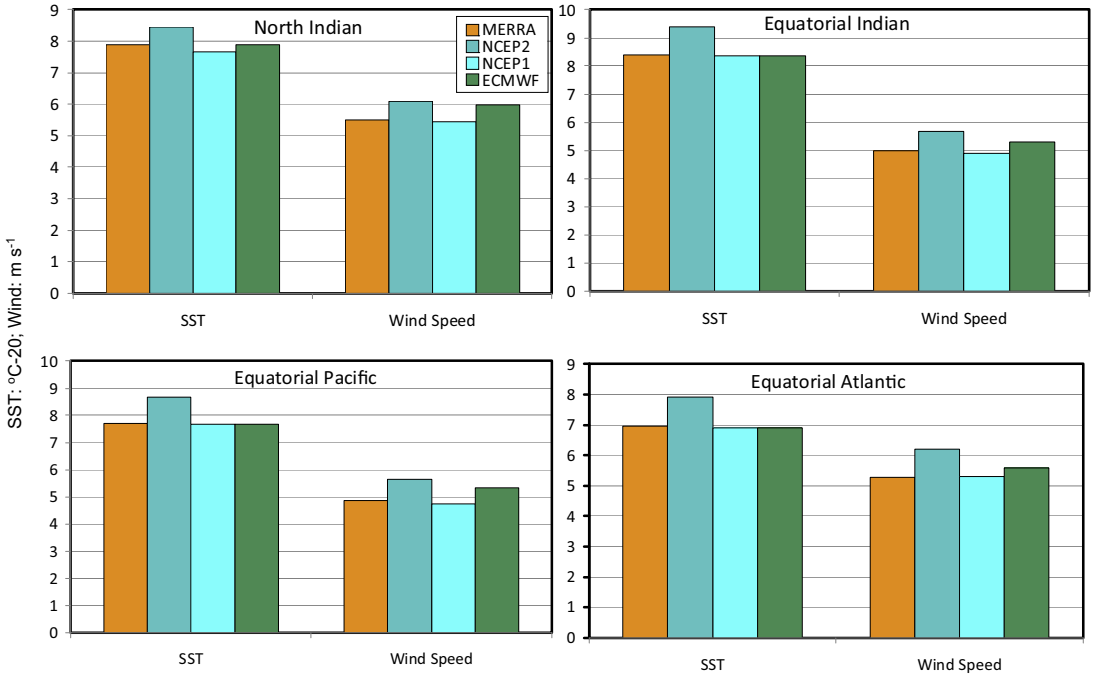

Fig. 10. Annual mean SST (degrees C – 20,), and wind speeds (m s^{-1}) for the 4 reanalysis products in the tropical basins. Note that SST is subtracted by 20° to fit on the same scale as wind speed.

the four reanalysis products, global ocean carbon mean fluxes and pCO_2 are insensitive to them. This is less sweeping when one considers that only a portion of the vast reanalysis variables produced are important in ocean carbon modeling, the most important of which are surface temperature, wind speeds and stresses, and ice distributions, and when the sensitivities of ocean carbon models are determined by complex interactions in the model formulations.

Although the global carbon flux and pCO_2 distributions are similar among reanalyses, there are considerable differences on oceanographic basin scales. Air–sea carbon fluxes, which, as small differences between large values of atmospheric and ocean pCO_2, are especially sensitive to small variations in the representation of atmospheric forcing by reanalysis products. None of the reanalysis products are uniformly superior in all basins, nor are any uniformly inferior, as compared to in situ estimates. The differences among the reanalyses are largest in the high latitudes and the tropics, which incidentally represent the basins of strongest sinks and strongest sources, respectively.

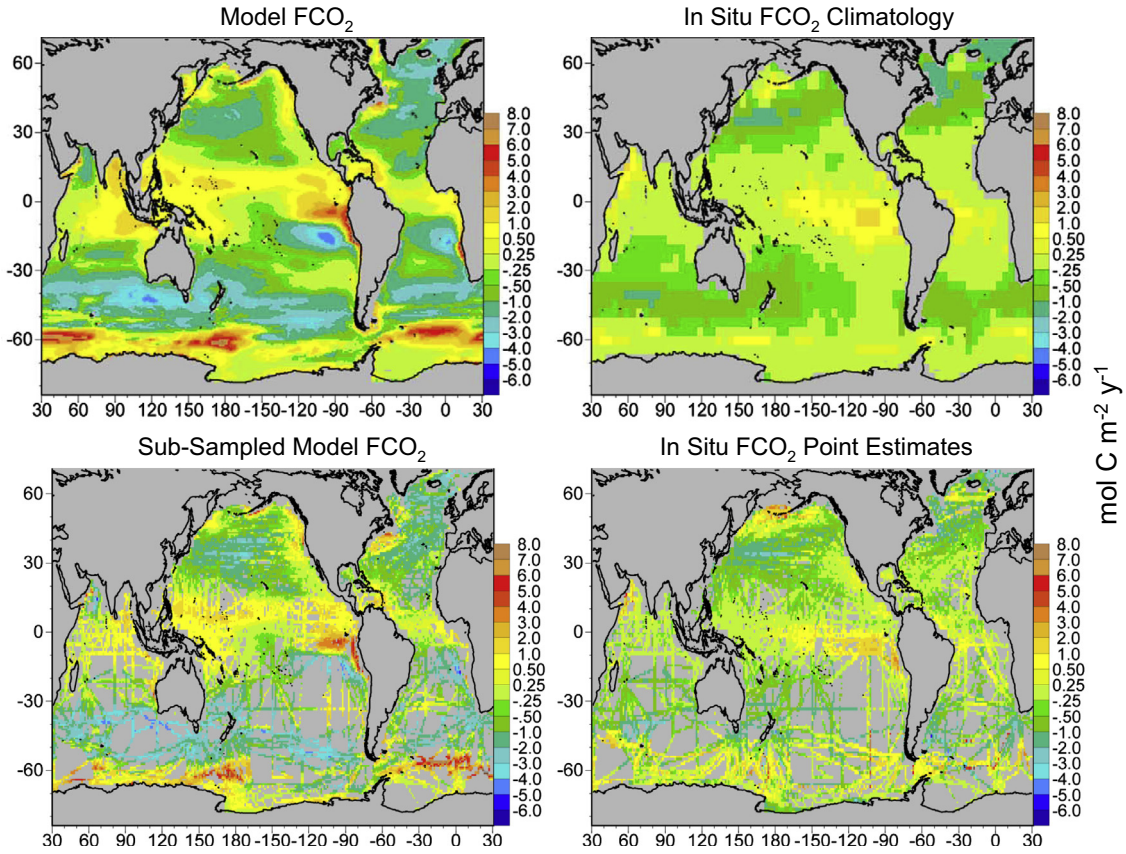

Fig. 11. Model and in situ FCO_2 (top), and sub-sampled model corresponding to point measurements in situ FCO_2 (bottom). The model is represented by the MERRA-forced version. The model is sub-sampled by month and location to the in situ data to produce a comparable annual mean.

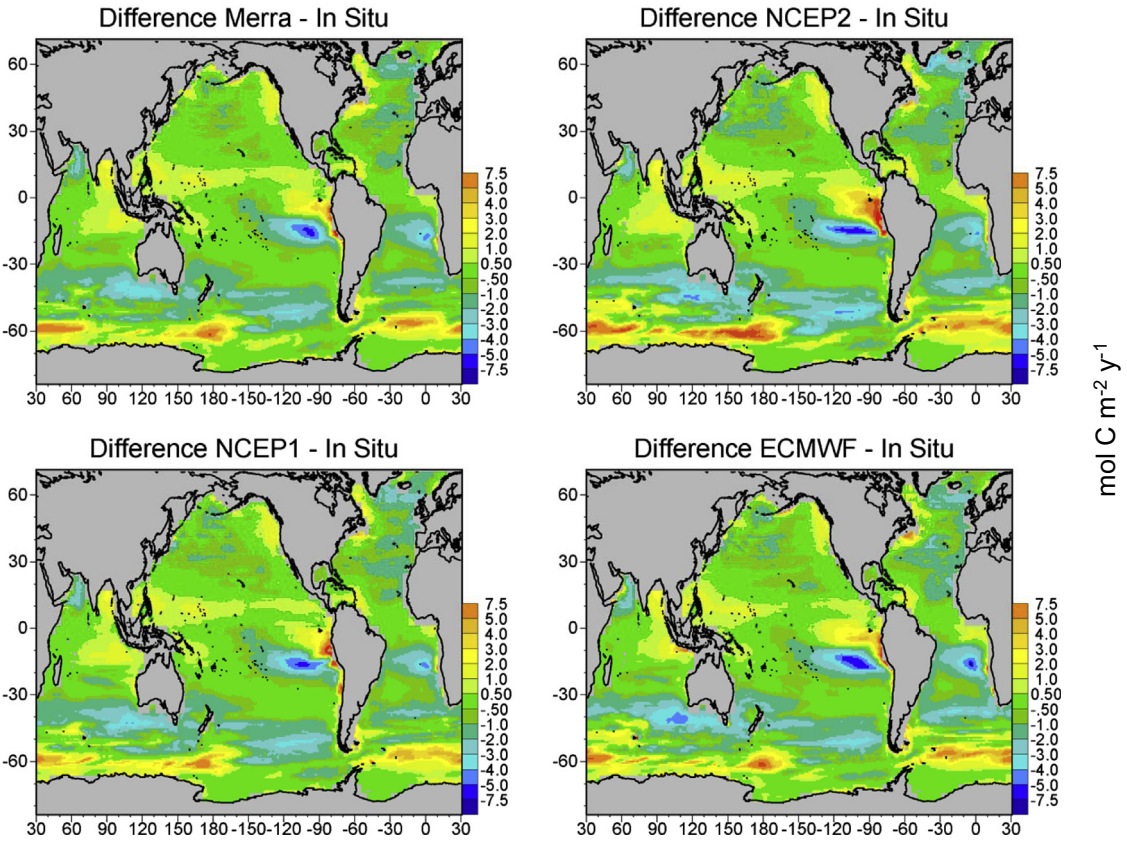

Fig. 12. Difference in model forcing by the four different reanalysis products and in situ FCO_2.

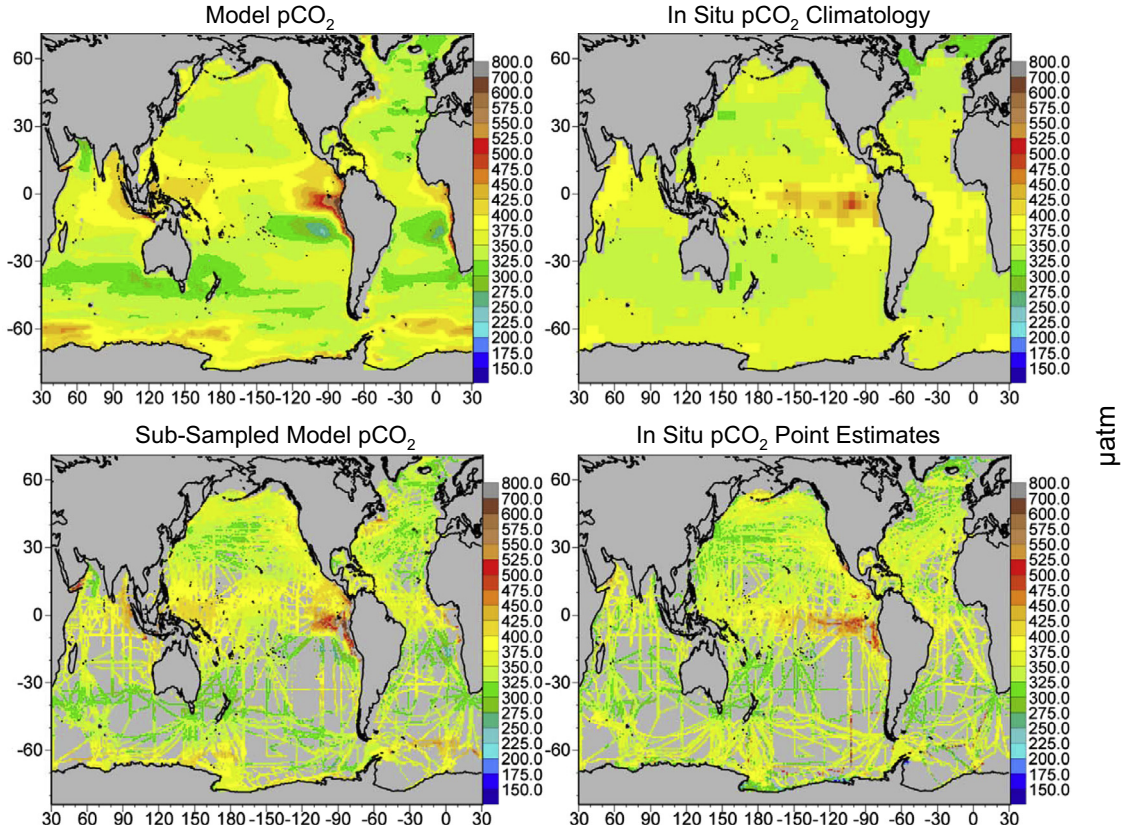

Fig. 13. Model and in situ gridded pCO_2 (top), and sub-sampled model corresponding to point measurements in situ pCO_2 (bottom). The model is represented by the MERRA-forced version. The model is sub-sampled by month and location to the in situ data to produce a comparable annual mean.

Few of the major departures observed in MERRA forcing, such as the South Atlantic and Pacific, North Indian, North Central Pacific, and North Pacific, are rectified by the other reanalysis products (Fig. 5). ECMWF forcing, however, substantially ameliorates the departures observed in the MERRA and NCEP forcings in the North Indian and the Equatorial Pacific.

Attribution of the differences of air–sea fluxes to specific variables in the reanalysis products is difficult because of the complexity of the ocean carbon cycle. Additionally, differences in annual mean fluxes shown here can be the result of seasonal differences in reanalysis products. A complete analysis of the effects of the reanalysis products and their influences on the representation of the global ocean carbon cycle is beyond the scope of this paper. However, it is worthwhile to attempt to relate differences in forcing with differences in fluxes, at least at coarse basin and annual scales, to assist in understanding how the reanalysis variables are affecting the observed changes in the representation of the global ocean carbon cycle.

First, we note that there are really only 6 reanalysis variables affecting the air–sea fluxes in this biogeochemical model: ice concentrations, SST, surface pressure, wind speeds, and the x and y components of wind stress (Fig. 1). We can partially separate these into those that (1) affect the circulation, and therefore affect the biology, chemistry, and physical transfers of carbon in the water column and producing the surface distributions where the exchange with the atmosphere occur (SST and wind stress), and (2) those that directly affect the exchange of carbon between the ocean and atmosphere (sea ice, wind speeds and pressure). Here we restrict our investigation to SST, sea ice, and wind speeds. Pressure plays a modest role in the air–sea flux and the differences among the reanalysis products is relatively small. Wind stresses are critical drivers of the circulation patterns and vertical processes, but they operate in complex ways and much of their influence is reflected in the SST.

Beginning with the high latitudes, the Antarctic basin exhibits a very large range of estimated fluxes from the different reanalysis products (Fig. 5), with NCEP2 producing a much lower sink than the other reanalyses. The NCEP2 reanalysis coincidentally has the highest SST (>1 °C higher than the lowest from ECMWF), and the highest wind speeds (1.4 m s^{-1} higher than the lowest, represented by NCEP1), as seen in Fig. 6. The higher temperature from NCEP2 coupled with stronger winds is consistent with stronger outgassing of CO_2 in the Antarctic, which would produce a reduced basin scale sink, as observed here.

In the northern high latitudes, MERRA forcing produces the weakest sinks, which correspond with relatively low wind speeds (Fig. 9). MERRA winds are >1 m s^{-1} lower than the highest winds in both the North Pacific and North Atlantic. These low winds in MERRA are consistent with reduced exchange of pCO_2 with the atmosphere and result in reduced sinks of atmospheric carbon. The relatively high SST of MERRA may also play a role in weakening the North Atlantic fluxes. Similarly, we note that the strongest sinks in the North Atlantic are produced by NCEP2 and NCEP1. NCEP2 has the strongest winds, while NCEP1 has the lowest SST's.

The tropical basins produce the largest range in air–sea carbon fluxes among the 4 reanalysis products (Figs. 5 and 6). The most notable divergences are NCEP2 (strongest source) and MERRA (weakest source) in the Equatorial Pacific. NCEP2 SST and wind speeds are both the largest of the reanalyses (Fig. 10). NCEP2 SST is >1 °C higher than the lowest (ECMWF, although NCEP1 and MERRA are consistent to within 0.03 °C), and NCEP2 wind speed is 0.9 m s^{-1} higher than the lowest, represented by NCEP1. These high SST's and wind speeds can be associated with stronger outgassing as observed in the fluxes. The converse is true as well:

NCEP1's and MERRA's weaker winds produce lower fluxes, despite high pCO_2 than the data (Fig. 7). A similar series of observations occur in the Equatorial Atlantic, with NCEP2's stronger representation of a source to the atmosphere (Fig. 5) is associated with the highest SST and wind speed (Fig. 10). The weakest source produced by MERRA forcing in these two basins is more difficult to attribute to MERRA's representation of SST and wind speed.

4.2. Inherent model/data issues

Although not the primary focus of this effort, the intercomparison of simulated fluxes and pCO_2 from four different reanalysis products provides an opportunity to gain insights into inherent model and data ocean carbon issues. First we note that the reanalysis products are largely not capable of rectifying the major discrepancies between the model and data. Second we note that as we descend from coarser to finer resolution, the issues become more important.

For both air–sea fluxes and pCO_2, global model agreement with in situ data is strong, with maximum deviations of 19% for FCO_2 and 0.6% for pCO_2 among all the reanalysis forcing products (Figs. 5 and 7). Deviations for pCO_2 are much smaller than fluxes. Basin correlations are statistically significant at $P < 0.05$ for all forcings for both FCO_2 and pCO_2, and correlation coefficients range from 0.73 to 0.80.

On regional scales, more model-data deviations are apparent and they can be large at times. We note particularly the South Atlantic and to a lesser extent the North Atlantic (Figs. 5 and 7). For air–sea fluxes, additional problems are seen in the Pacific basins (except the Equatorial Pacific) and the Equatorial Atlantic. pCO_2 estimates exhibit much smaller discrepancies in the above basins but not in the North and South Atlantic (Fig. 7). Since the results from the different forcings only partially alleviate the model-data differences, we suggest that here the problems arise in the model formulation and/or the comparison with in situ data.

On smaller scales the discrepancies between model and data are larger still (Figs. 11 and 12). For the full model domain and interpolated in situ climatology (top panels in Fig. 11), noteworthy deviations are the high source regions in the model in the Southern Ocean along the 60°S band, high sources along the US/Canada East and West coasts in the North Atlantic and Pacific, and model sinks in the southern sub-tropical Atlantic and Pacific.

The 60°S Southern Ocean band of high atmospheric source is common to all the reanalysis versions, and the discrepancy is partially the result of sampling biases in the in situ data. Public data sets of pCO_2 and FCO_2 (Takahashi et al., 2009) are taken from point measurements in the ocean, gridded to 5° longitude by 4° latitude, binned to an annual mean climatology, and with residual gaps filled. Each of these steps potentially introduces a bias in the final result, and is especially important when comparing to model annual means, which have no sampling issues. Binning to a coarse grid reduces variability and over-represents the influences of observation points closest to gaps. Constructing annual means where data exist for only a few months creates an unbalanced representation, with the sampled months over-represented. If the sampled months occur at a low or high point in the seasonal cycle, the problem is exacerbated. Filling gaps, like binning to a coarse grid, over-represents the influence of observations nearest the gaps unless methods are actively used to reduce this problem. Takahashi et al. (2009) used an interpolation scheme based on assumed advective transport.

When we sub-sample the model to match the point measurement locations and months observed, and construct a model representation of data corresponding in time and space to the data, we see that the areas of high sources along 60°S are considerably reduced in intensity and extent (Fig. 11). The localized high source region from longitudes 20°E to 75°E nearly disappears. Now, the reduction and disappearance does not mean that the model agrees with data. We note that there is some evidence of outgassing in the data in this region, such as the portion just north and slightly west of the Ross Sea, and in the central Atlantic sector. However, the residual disagreement between the sub-sampled model and data points to model issues. The outgassing in the model, and to a lesser extent the data, is intensified in austral autumn and winter. This corresponds with high pCO_2 (data not shown), resulting from convection of deep DIC and low ocean temperatures. The model is not capable of sequestering carbon uptake and sinking by biological processes in austral summer deep enough to avoid return to the surface in local winter. We note that other models exhibit outgassing along this 60°S band as well (e.g., Doney et al., 2009), but they are admittedly less intense and less widespread than seen here.

A similar explanation helps explain the discrepancies between the model and data in the South Atlantic. Poor sampling produces a distorted view of the model-data comparison in the interpolated representations. In the sub-sampled model, the correspondence is improved (Fig. 11), although there are mismatches along two north–south lines toward the eastern portion of the basin. In fact, the basin mean model-data flux difference here falls from -1.17 mol m^{-2} y^{-1} in the full interpolated data and model to -0.18 mol m^{-2} y^{-1} in the sub-sampled representation.

Data sampling issues also contribute to the discrepancies in the South Pacific. Here the basin mean model-data flux bias is -0.45 mol m^{-2} y^{-1} for the interpolated comparison (Fig. 5). When the sampling biases are removed the difference is nearly half at 0.27 mol m^{-2} y^{-1}.

Model-data biases in the North Atlantic and Pacific are more complicated. Some of the difference is due to data sampling, as the LDEO data are missing in the northern Labrador Sea and the Sea of Okhotsk. But otherwise data sampling in these two basins is relatively complete spatially and temporally. The near-coastal source regions in the model near the US/Canada borders are in contrast to the data and suggest model formulation issues. Since the discrepancies appear in all the reanalysis versions (although variable), they are apparently not due to differences in forcing. The possibility of issues in winds, SST, and ice common across all the reanalysis products cannot be ignored, but we ascribe (1) excessive upwelling coupled with excessive deep carbon in the model, (2) locally high atmospheric pCO_2 from fossil fuel burning that is not represented in the global mean value used, and (3) inadequate uptake and sequestration of carbon by biological processes.

The Equatorial Atlantic also exhibits large model-data discrepancies in fluxes (Fig. 5). This is one of the most perplexing basins, since the model pCO_2 results, by all the forcings, are consistent with data: ECMWF and MERRA are within 5 μatm (1.2%) while the two NCEP forcings are within 1 μatm (0.2%) (Fig. 7). Fluxes are a non-linear function of pCO_2 (actually delta pCO_2), with functions involving wind speed and temperature contributing to the non-linearity (Wanninkhof, 1992). Small differences in these variables may produce large changes in the fluxes. It is important to remember that the LDEO air–sea fluxes are estimates derived from observed ΔpCO_2 and estimated wind speeds, along with a gas transfer coefficient (Takahashi et al., 2009). Gröger and Mikolajewicz (2011) have suggested that the Schmidt number for flux estimates (involved in the gas transfer coefficient) could have issues at temperatures > 30 °C, but neither the sea surface temperature climatologies used by LDEO (from Conkright et al., 2002) or the SST climatologies in our reanalysis data ever exceed this threshold in the Equatorial Atlantic. Additionally, our use of this parameter is the same as for the in situ estimates (Takahashi et al., 2009). As with several other basins, when we account for sampling, the disparity in fluxes is much smaller. The in situ flux estimates decline by nearly half, from 0.63 to 0.33 mol C m^{-2} y^{-1}.

This produces in situ flux estimates similar to the NCEP2 fluxes shown in Fig. 5. MERRA-forced model fluxes sampled to the in situ estimates (Fig. 11) decline only about 0.07 mol C m^{-2} y^{-1}, so they remain essentially the same as shown in Fig. 5 for this basin. This means that when sampling biases are removed, the difference between MERRA-estimated fluxes and in situ estimates is about the same as the difference between the model forced by MERRA and by NCEP2. Residual differences are likely due to wind speed resolution differences (we interpolate reanalysis data to the native model grid, 1.25° longitude by 0.67° latitude, compared to the NCEP2 reanalysis re-gridded to 5° longitude by 4° latitude resolution by LDEO). When we interpolate our NCEP2 wind speed reanalysis data over the LDEO resolution, we find a mean increase of 1.86 m s^{-1} in the Equatorial Atlantic, which would lead to enhanced atmosphere–ocean carbon exchange. Re-gridding can be sensitive to data frequency distributions, especially in small basins such as this one. It can also increase the influence of values over land, which may affect the representation of the mean wind speeds.

5. Summary and conclusions

Intercomparison of air–sea carbon fluxes and pCO_2 spatial distributions using a single ocean model and four different reanalysis products shows that global means are insensitive to the choice of reanalysis product. This suggests that at least for the variables most important for ocean carbon exchange, i.e., wind speeds, SST, and ice, the reanalysis products are either in general agreement, or that the differences among them are relatively unimportant at the largest spatial scales. This finding is emphatically not true for regional analyses, where large differences in FCO_2 are observed depending upon the reanalysis product used for forcing. pCO_2 distributions are considerably less sensitive to the choice of reanalysis product. These findings have important implications for ocean modelers in choosing reanalysis products: namely that for global models it does not matter much, but for regional and local model the selection can have important influences on carbon cycling and exchange estimates.

The finding that different estimates of air–sea fluxes are produced by different reanalyses at regional scales reinforces the work by Otero et al. (2013), who used different reanalysis sources in the Bay of Biscay. Several other ocean carbon modeling efforts have utilized versions of NCEP forcing data (e.g., Le Quéré et al., 2010; Doney et al., 2009; McKinley et al., 2004).

This effort provides a milepost for evaluating the use of different reanalysis forcing products for ocean carbon models, at least in a general sense. The overarching conclusion, i.e., that global estimate of carbon fluxes and pCO_2 are insensitive to the choice of forcing is likely robust. Similarly the other conclusions that regionally and sub-regionally the choice of reanalysis has successively more influence, is also likely to apply to other models as well. However the nature of the differences and sensitivities is likely to be different. The difference will be dependent upon the nature of the model formulation, but we hope the results provided here will be of help in the selection and use of reanalysis products for global and regional ocean carbon models.

Acknowledgements

We thank the NASA/MERRA Project, the NOAA/NCEP Project and the ECMWF Project for the data sets and public availability. We also thank the Lamont-Doherty Earth Observatory for in situ pCO_2 data and flux estimates. We thank three anonymous reviewers for insights. This work was supported by NASA Modeling and Analysis Program (MAP) and Carbon Monitoring System (CMS) Programs.

References

Conkright, M.E., Garcia, H.E., O'Brien, T.D., Locarnini, R.A., Boyer, T.P., Stephens, C., Antonov, J.I., 2002. World ocean atlas 2001, volume 4: nutrients. In: Levitus, S. (Ed.), NOAA Atlas NESDIS 52. U.S. Government Printing Office, Wash., DC, p. 392.

Dee, D.P. et al., 2011. The ERA-Interim reanalysis: configuration and performance of the data assimilation system. Q. J. R. Meteorol. Soc. 137, 553–597.

Doney, S.C. et al., 2009. Mechanisms governing interannual variability in upper-ocean inorganic carbon system and air–sea CO_2 fluxes: physical climate and atmospheric dust. Deep Sea Res. II 56, 640–655.

Field, C.B., Behrenfeld, M.J., Randerson, J.T., Falkowski, P., 1998. Primary production of the biosphere: integrating terrestrial and oceanic components. Science 281, 237–240.

Ginoux, P., Chin, M., Tegen, I., Prospero, J.M., Holben, B., Dubovik, O., Lin, S.-J., 2001. Sources and distributions of dust aerosols simulated with the GOCART model. J. Geophys. Res. 106, 20255–20273.

Gorgues, T., Aumont, O., Rodgers, K.B., 2010. A mechanistic account of increasing seasonal variations in the rate of ocean uptake of anthropogenic carbon. Biogeosciences 7, 2581–2589.

Gregg, W.W., Casey, N.W., 2007. Modeling coccolithophores in the global oceans. Deep Sea Res. II 54, 447–477.

Gregg, W.W., Ginoux, P., Schopf, P.S., Casey, N.W., 2003. Phytoplankton and iron: validation of a global three-dimensional ocean biogeochemical model. Deep Sea Res. II 50, 3143–3169.

Gregg, W.W., Casey, N.W., Rousseaux, C.S., 2013. Global surface ocean carbon estimates in a model forced by MERRA. NASA Global Modeling and Assimilation Series, M. Suarez, ed., NASA Technical Memorandum 2012–104606, Vol. 31, 32 pp.

Gröger, M., Mikolajewicz, U., 2011. Note on the CO_2 air–sea gas exchange at high temperatures. Ocean Modell. 39, 284–290.

Kalnay, E., Kanamitsu, M., Kistler, R., Collins, W., Deaven, D., Gandin, L., Iredell, M., Saha, S., White, G., Woollen, J., Zhu, Y., Chelliah, M., Ebisuzaki, W., Higgins, W., Janowiak, J., Mo, K.C., Ropelewski, C., Wang, J., Leetmaa, A., Reynolds, R., Jenne, Roy, Joseph, D., 1996. The NCEP/NCAR 40-year reanalysis project. Bull. Am. Meteorol. Soc. 77, 437–471.

Kanamitsu, M., Ebisuzaki, W., Woollen, J., Yang, S.K., Hnilo, J.J., Fiorino, M., Potter, G.L., 2002. NCEP-DOE-AMIP-II reanalysis (R-2). Bull. Am. Meteorol. Soc., 1631–1643.

Kaufman, Y.J., Herring, D.D., Ranson, K.J., Collatz, G.J., 1998. Earth observing system AM1 mission to Earth. IEEE Trans. Geosci. Remote Sens. 36, 1045–1055.

Key, R.M., Kozyr, A., Sabine, C.L., Lee, K., Wanninkhof, R., Bullister, J.L., Feely, R.A., Millero, F.J., Mordy, C., Peng, T.-H., 2004. A global ocean carbon climatology: results from global data analysis project (GLODAP). Global Biogeochem. Cycles 18. http://dx.doi.org/10.1029/2004GB002247.

Khatiwala, S. et al., 2013. Global ocean storage of anthropogenic carbon. Biogeosciences 10, 2169–2191.

Le Quéré, C., Takahashi, T., Buitenhuis, E.T., Rodenbeck, C., Sutherland, S.C., 2010. Impact of climate change and variability on the global oceanic sink of CO_2. Global Biogeochem. Cycles 24, GB4007. http://dx.doi.org/10.1029/2009GB003599.

McKinley, G.A., Rodenbeck, C., Gloor, M., Houweling, S., Heimann, M., 2004. Pacific dominance to global air–sea CO_2 flux variability: a novel atmospheric inversion agrees with ocean models. Geophys. Res. Lett. 31, L22308. http://dx.doi.org/10.1029/2004GL021069.

McKinley, G.A., Takahashi, T., Buitenhuis, E., Chai, F., Christian, J.R., Doney, S.C., Jiang, M.-S., Lindsay, K., Moore, J.K., Le Quéré, C., Lima, I., Murtugudde, R., Shi, L., Wetzel, P., 2006. North Pacific carbon cycle response to climate variability on seasonal to decadal timescales. J. Geophys. Res. 111, C07S06. http://dx.doi.org/10.1029/2005JC003173.

Otero, P., Padin, X.P., Ruiz-Villarreal, M., Garcia-Garcia, L.M., Rios, A.F., Perez, F.F., 2013. Net sea–air CO_2 flux uncertainties in the Bay of Biscay based on the choice of wind speed products and gas transfer parameterizations. Biogeosciences 10, 2993–3005.

Rienecker, M.M. et al., 2011. MERRA – NASA's modern-era retrospective analysis for research and applications. J. Climate 24, 3624–3648. http://dx.doi.org/10.1175/JCLI-D-11- 00015.1.

Schopf, P.S., Loughe, A., 1995. A reduced gravity isopycnal ocean model: Hindcasts of El Nino. Mon. Weather Rev. 123, 2839–2863.

Takahashi, T., Sutherland, S.C., Feely, R.A., Wanninkhof, R., 2006. Decadal change of the surface water pCO_2 in the North Pacific: a synthesis of 35 years of observations. J. Geophys. Res. 111, C07S05. http://dx.doi.org/10.1029/2005JC003074.

Takahashi, T. et al., 2009. Climatological mean and decadal change in surface ocean pCO_2, and net sea–air CO_2 flux over the global ocean. Deep Sea Res. II 56, 554–577.

Wanninkhof, R., 1992. Relationship between wind speed and gas exchange over the ocean. J. Geophys. Res. 97 (C5), 7373–7382.